†Supporting information

Measuring Pb, Th, and U inter-element ratios in geological materials using extreme ultraviolet laser ablation and ionization mass spectrometry

Lydia A. Rush[a]*, Andrew M. Duffin[b] and Carmen S. Menoni[a]

[a]*Department of Electrical and Computer Engineering, Colorado State University, Fort Collins, CO 80523, USA*

[b]*National Security Directorate, Pacific Northwest National Laboratory, Richland, WA 99352, USA*

**Corresponding author: lrush@colostate.edu, Tel: +1 970 4918519*

Table S1 Expected/literature mass fractions (in µg/g) of Pb, Th, and U and their respective 1 standard deviation (±1SD) uncertainties for the samples investigated in this study. The mass fractions and their associated uncertainties listed for the synthetic glasses (NIST610, USGS GSE-1G and STDP5) and iron manganese (FeMnOx-1) material were used to calculate the $^{206}Pb/^{238}U$ and $^{232}Th/^{238}U$ ratio values found in the main text in Table 1. (Mass fractions for most samples can be found in the GeoRem Database: http://georem.mpch-mainz.gwdg.de/; mass fraction measurements for SR1, EA, 14971, SL-B, Mogok 2A, Mogok 2C, and Mogok 1 were directly provided by the USGS and are readily available to readers upon request via the corresponding author's email address).

Sample	Pb_{total}	±1SD	^{206}Pb	±1SD	^{232}Th	±1SD	U_{total}	±1SD	^{238}U	±1SD
NIST610	426	1	102.7*	0.2	457.2	1.2	461.5	1.1	460.4	1.1
USGS GSE-1G	378	12	91*	3	380	20	420	30	417*	30
STDP5	1414	61.5	341*	15	1235	133	1378	5	1368*	5
FeMnOx-1	1624	280	391*	67	534	40	547	17	543*	17
SR1	n/a	n/a	218**	3	185	4	n/a	n/a	2455	35
EA	n/a	n/a	70**	1	292	8	n/a	n/a	803	15
14971										
LA ICP-MS	n/a	n/a	173*	3	37819	2404	n/a	n/a	1141	22
ID-TIMS	1904	94	238	13	41914	2335	1580	90	1569	89
Bananeira†	n/a	n/a	243	40	68252	5574	n/a	n/a	972	179
Diamantina†	n/a	n/a	93	11	3588	1822	n/a	n/a	355	41
SL-B	n/a	n/a	29688**	618	543556	7088	n/a	n/a	277039	5732
Mogok 2A	n/a	n/a	3735**	25	528320	2270	n/a	n/a	341808	2266
Mogok 2C	n/a	n/a	4716**	46	418880	4480	n/a	n/a	450034	4421
Mogok 1	n/a***	n/a	n/a***	n/a	24310	2101	n/a	n/a	290841	3683

*Calculated ^{206}Pb and ^{238}U mass fractions from total Pb and U content, respectively, assuming natural isotopic abundance. (Note: The $^{206}Pb/^{208}Pb$ ratio has been measured for USGS GSE-1G using LA ICP-MS and SIMS, obtaining a ratio value of approximately 1.96,[1,2] whereas the natural $^{206}Pb/^{208}Pb$ ratio is 2.17. Nonetheless, the natural Pb abundance was assumed here because the measured isotope abundance was not directly available)

**Calculated radiogenic Pb mass fractions from direct ratio measurements of $^{206}Pb/^{238}U$ and mass fraction measurements of ^{238}U

***Sample has too high common Pb to give calculated Pb content

†Mass fraction values measured with LA Q-ICP-MS[3, 4]

Table S2 The ion counts of ^{206}Pb, ^{232}Th, ^{238}U, $^{232}Th^{16}O$, $^{238}U^{16}O$, $^{232}Th^{16}O_2$, and $^{238}U^{16}O_2$ measured with the EUV TOF in each super crater ablated on the samples analyzed in this study. The corresponding Pb/U and Th/U ratios for each super crater with its ±2σ uncertainty is also listed, where the ratio considers all oxide species detected in the super crater, unless otherwise specified. The weighted average of the Pb/U and Th/U ratios is also shown alongside the ±2σ uncertainty, which is calculated using the equations in Table S3.

Sample: NIST 610 (silicate glass)

	Measured Counts							***Measured Ratios***			
Super crater #	^{206}**Pb**	^{232}**Th**	^{238}**U**	^{232}**Th**^{16}**O**	^{238}**U**^{16}**O**	^{232}**Th**^{16}**O$_2$**	^{238}**U**^{16}**O$_2$**	**Pb/U**	**±2σ**	**Th/U**	**±2σ**
1*	58	316	250	274	264	n/a	60	0.101	0.03	1.03	0.17
2*	55	332	278	304	284	n/a	62	0.089	0.03	1.02	0.17
3*	64	249	191	240	208	n/a	59	0.140	0.04	1.07	0.20
4*	77	322	243	307	280	n/a	47	0.136	0.04	1.10	0.19
5*	83	377	336	286	270	n/a	69	0.123	0.03	0.98	0.15
6*	82	408	324	276	258	n/a	66	0.127	0.03	1.06	0.16
7	44	174	90	193	167	n/a	78	0.131	0.05	1.10	0.24
8	44	119	59	147	148	n/a	68	0.161	0.06	0.97	0.27
9	44	113	90	136	125	n/a	81	0.149	0.05	0.84	0.22
10	47	97	88	100	94	n/a	68	0.189	0.07	0.79	0.23
11	44	71	67	111	98	n/a	77	0.184	0.07	0.75	0.25
12	39	52	50	63	78	n/a	69	0.200	0.08	0.58	0.24
13	42	42	49	68	57	n/a	53	0.267	0.11	0.70	0.31
14*	127	729	651	539	479	n/a	66	0.106	0.02	1.06	0.12
15*	133	724	628	489	480	n/a	74	0.112	0.02	1.02	0.12
16*	137	662	555	485	483	n/a	77	0.123	0.03	1.03	0.12
17*	167	906	809	676	693	n/a	126	0.102	0.02	0.97	0.09
18*	168	809	764	637	619	n/a	119	0.112	0.02	0.96	0.09
19*	169	849	726	707	654	n/a	122	0.113	0.02	1.04	0.10
Weighted average of ratios								**0.112**	**0.007**	**0.99**	**0.03**

*Values used in the calculation of the Pb/U weighted average ratio because these runs have total U counts >400.

Sample: USGS GSE-1G (basalt glass)

	Measured Counts							Measured Ratios			
Super crater #	**^{206}Pb**	**^{232}Th**	**^{238}U**	**$^{232}Th^{16}O$**	**$^{238}U^{16}O$**	**$^{232}Th^{16}O_2$**	**$^{238}U^{16}O_2$**	**Pb/U**	**±2σ**	**Th/U**	**±2σ**
1	195	919	955	785	779	n/a	136	0.104	0.02	0.91	0.08
2	234	942	1078	809	785	n/a	174	0.115	0.02	0.86	0.07
3	228	954	981	760	794	n/a	175	0.117	0.02	0.88	0.07
Weighted average of ratios								**0.11**	**0.01**	**0.88**	**0.04**

Sample: STDP5 (phosphate glass)

	Measured Counts							Measured Ratios			
Super crater #	**^{206}Pb**	**^{232}Th**	**^{238}U**	**$^{232}Th^{16}O$**	**$^{238}U^{16}O$**	**$^{232}Th^{16}O_2$**	**$^{238}U^{16}O_2$**	**Pb/U**	**±2σ**	**Th/U**	**±2σ**
1	420	1585	1347	1375	1411	n/a	477	0.13	0.01	0.91	0.05
2	386	1539	1227	1401	1373	n/a	498	0.12	0.01	0.95	0.06
3	414	n/a*	1281	1350	1409	n/a	468	0.13	0.01	n/a	n/a
4	662	2456	2289	1817	1779	n/a	353	0.15	0.01	0.97	0.05
5	393	1179	995	1013	992	n/a	365	0.17	0.02	0.93	0.06
6	309	1006	945	986	926	n/a	347	0.14	0.02	0.90	0.07
Weighted average of ratios								**0.138**	**0.006**	**0.94**	**0.04**

*^{232}Th signal could not be resolved from ringing induced by a large peak at m/z = 231

Sample: FeMnOx-1 (iron manganese oxide powder)

	Measured Counts							Measured Ratios			
Super crater #	**^{206}Pb**	**^{232}Th**	**^{238}U**	**$^{232}Th^{16}O$**	**$^{238}U^{16}O$**	**$^{232}Th^{16}O_2$**	**$^{238}U^{16}O_2$**	**Pb/U**	**±2σ**	**Th/U**	**±2σ**
1	674	1228	1165	462	426	n/a	n/a	0.42	0.04	1.06	0.07
2	500	831	717	439	378	n/a	n/a	0.46	0.04	1.16	0.10
3	399	703	656	429	356	n/a	n/a	0.39	0.04	1.12	0.10
Weighted average of ratios								**0.42**	**0.02**	**1.10**	**0.05**

Sample: SR1 (zircon)

	Measured Counts							*Measured Ratios*			
Super crater #	**^{206}Pb**	**^{232}Th***	**^{238}U**	**$^{232}Th^{16}O$**	**$^{238}U^{16}O$**	**$^{232}Th^{16}O_2$**	**$^{238}U^{16}O_2$**	**Pb/U**	**±2σ**	**Th/U**	**±2σ**
1	500	Interf.	4865	492	6179	n/a	2396	0.037	0.003	0.080	0.007
2	431	Interf.	3706	385	5481	n/a	2058	0.038	0.004	0.070	0.007
3	414	Interf.	2669	338	4667	n/a	1919	0.045	0.004	0.072	0.008
Weighted average of ratios								**0.039**	**0.002**	**0.074**	**0.004**

*^{232}Th signal had interference (interf.) from $^{92}Zr_2{}^{16}O_3$ at m/z = 232, so only $^{232}Th^{16}O$ and $^{238}U^{16}O$ signals are used for the Th/U ratio

Sample: EA (zircon)

	Measured Counts							*Measured Ratios*			
Super crater #	**^{206}Pb***	**^{232}Th****	**^{238}U****	**$^{232}Th^{16}O$**	**$^{238}U^{16}O$**	**$^{232}Th^{16}O_2$**	**$^{238}U^{16}O_2$ *****	**Pb/U**	**±2σ**	**Th/U**	**±2σ**
1	n/a	Interf.	Intef.	235	729	n/a	472	n/a	n/a	0.32	0.05
2	n/a	Interf.	Interf.	241	671	n/a	502	n/a	n/a	0.36	0.05
3	n/a	Interf.	Interf.	177	577	n/a	457	n/a	n/a	0.31	0.05
Weighted average of ratios								**n/a**	**n/a**	**0.33**	**0.03**

*^{206}Pb was below EUV TOF detection limits; **^{232}Th signal had interference (interf.) from $^{92}Zr_2{}^{16}O_3$ and ^{238}U had interference from $^{94}Zr^{96}Zr^{16}O_3$;***$^{238}U^{16}O_2$ was not used for any ratio measurements, but the detected ion counts are shown here for reference.

Sample: 14971 (monazite)

	Measured Counts							*Measured Ratios*			
Super crater #	**^{206}Pb**	**^{232}Th**	**^{238}U**	**$^{232}Th^{16}O$**	**$^{238}U^{16}O$**	**$^{232}Th^{16}O_2$**	**$^{238}U^{16}O_2$**	**Pb/U**	**±2σ**	**Th/U**	**±2σ**
1	118	27041	806	15320	486	258	325	0.07	0.01	26.4	1
2	94	17317	505	10739	372	219	268	0.08	0.02	24.7	1
3	92	25344	677	13107	408	162	180	0.07	0.02	30.5	1
4	96	25481	779	12833	409	152	164	0.07	0.02	28.4	1
5	83	23818	826	11972	420	141	129	0.06	0.01	26.1	1
Weighted average of ratios								**0.071**	**0.007**	**26.8**	**0.5**

Sample: Bananeira (monazite)

	Measured Counts							*Measured Ratios*			
Super crater #	**^{206}Pb**	**^{232}Th**	**^{238}U**	**$^{232}Th^{16}O$**	**$^{238}U^{16}O$**	**$^{232}Th^{16}O_2$**	**$^{238}U^{16}O_2$**	**Pb/U**	**±2σ**	**Th/ U**	**±2σ**
1	87	57923	1661	28233	848	195	176	0.032	0.007	32.2	1
2	86	59232	1640	28013	904	171	139	0.032	0.007	32.6	1
3	74	57971	1703	28931	897	163	173	0.027	0.007	31.4	1
Weighted average of ratios								**0.030**	**0.004**	**32.0**	**0.7**

Sample: Diamantina-1 (monazite)

	Measured Counts							*Measured Ratios*			
Super crater #	**^{206}Pb**	**^{232}Th**	**^{238}U**	**$^{232}Th^{16}O$**	**$^{238}U^{16}O$**	**$^{232}Th^{16}O_2$**	**$^{238}U^{16}O_2$**	**Pb/U**	**±2σ**	**Th/U***	**±2σ**
1	43	1346	868	660	414	n/a	n/a	0.03	0.01	1.6	0.1
2	55	1800	911	966	506	n/a	n/a	0.04	0.01	2.0	0.1
3	77	1633	923	845	505	n/a	n/a	0.05	0.01	1.7	0.1
Weighted average of ratios								**0.041**	**0.006**	**1.74**	**0.06**

*Measured Th/U ratio is shown here only for reference because Th content is not homogenous in this sample (i.e., ID-TIMS measures Th/U ranging from 0.22 to 16.2)

Sample: SL-B (uraninite)

	Measured Counts							*Measured Ratios*			
Super crater #	**^{206}Pb**	**^{232}Th**	**^{238}U**	**$^{232}Th^{16}O$**	**$^{238}U^{16}O$**	**$^{232}Th^{16}O_2$**	**$^{238}U^{16}O_2$**	**Pb/U**	**±2σ**	**Th/U**	**±2σ**
1	23200	504047	297496	295621	142027	2074	51837	0.0472	6E-4	1.627	0.005
2	24273	517072	305737	303395	145600	2152	52238	0.0482	6E-4	1.629	0.005
3	24568	517426	304387	303324	143688	2230	52146	0.0491	6E-4	1.641	0.005
Weighted average of ratios								**0.0482**	**4E-4**	**1.633**	**0.003**

Sample: Mogok 2A (uraninite)

	Measured Counts							*Measured Ratios*			
Super crater #	^{206}**Pb**	^{232}**Th**	^{238}**U**	^{232}**Th**^{16}**O**	^{238}**U**^{16}**O**	^{232}**Th**^{16}**O**$_2$	^{238}**U**^{16}**O**$_2$	**Pb/U**	**±2σ**	**Th/U**	**±2σ**
1	6264	493398	317625	311687	165432	2707	62002	0.0115	3E-4	1.482	0.005
2	6479	488538	317485	318125	166445	2736	61050	0.0119	3E-4	1.485	0.005
3	6346	529630	335358	325728	163402	2549	57256	0.0114	3E-4	1.543	0.006
Weighted average of ratios								**0.0116**	**2E-4**	**1.503**	**0.003**

Sample: Mogok 2C (uraninite)

	Measured Counts							*Measured Ratios*			
Super crater #	^{206}**Pb**	^{232}**Th**	^{238}**U**	^{232}**Th**^{16}**O**	^{238}**U**^{16}**O**	^{232}**Th**^{16}**O**$_2$	^{238}**U**^{16}**O**$_2$	**Pb/U**	**±2σ**	**Th/U**	**±2σ**
1	7646	539295	443682	269825	204991	1465	68656	0.0107	2E-4	1.130	0.005
2	7101	442467	398372	282723	229631	2039	88310	0.0099	2E-4	1.015	0.004
3	7207	458963	407723	273318	224713	2010	82944	0.0101	2E-4	1.026	0.004
Weighted average of ratios								**0.0102**	**1E-4**	**1.051**	**0.002**

Sample: Mogok 1 (thorite)

	Measured Counts							*Measured Ratios*			
Super crater #	^{206}**Pb**	^{232}**Th**	^{238}**U**	^{232}**Th**^{16}**O**	^{238}**U**^{16}**O**	^{232}**Th**^{16}**O**$_2$	^{238}**U**^{16}**O**$_2$	**Pb/U**	**±2σ**	**Th/U**	**±2σ**
1	345	19316	211434	22249	241916	n/a	131263	0.00059	6E-5	0.071	0.001
2	305	15162	167792	18895	206792	n/a	123775	0.00061	7E-5	0.068	0.001
3	268	15066	167220	19490	207045	n/a	120478	0.00054	7E-5	0.070	0.001
Weighted average of ratios								**0.00058**	**4E-5**	**0.0698**	**6E-4**

Table S3 Equations used for calculating the weighted average of the ratios. The equations below specifically represent calculations for $^{206}Pb/^{238}U$ ratios. For $^{232}Th/^{238}U$ ratio calculations, ^{206}Pb is replaced with ^{232}Th ion counts. Eqtns. (5) and (6) are bold and represent the final ratio values *c* and their uncertainty σ, respectively, reported in the main text.

Eqtn. (1)	$Ratio = a_n = \frac{[206Pb\ (counts)]}{[238U\ (counts)]}$
Eqtn. (2)	$Ratio\ uncertainty = \delta_n = \frac{[206Pb\ (counts)]}{[238U\ (counts)]} * \sqrt{\left(\frac{1}{206Pb\ (counts)} + \frac{1}{238U\ (counts)}\right)}$
Eqtn. (3)	$Ratio\ weight = b_n = \frac{\frac{[206Pb\ (counts)]}{[238U\ (counts)]}}{\delta_n^2}$
Eqtn. (4)	$Ratio\ uncertainty\ weight = \alpha_n = \frac{1}{\delta_n^2}$
Eqtn. (5)	$Weighted\ average\ ratio = c = \frac{\sum(b1, b2 \ldots bn)}{\sum(\alpha 1,\ \alpha 2, \ldots \alpha n)}$
Eqtn. (6)	$Weighted\ uncertainty\ of\ ratio = \sigma = \sqrt{\frac{1}{\sum(\alpha 1, \alpha 2, \ldots \alpha n)}}$

Where n = 1,2,3,…n+1 and represents each ratio measured on the sample.

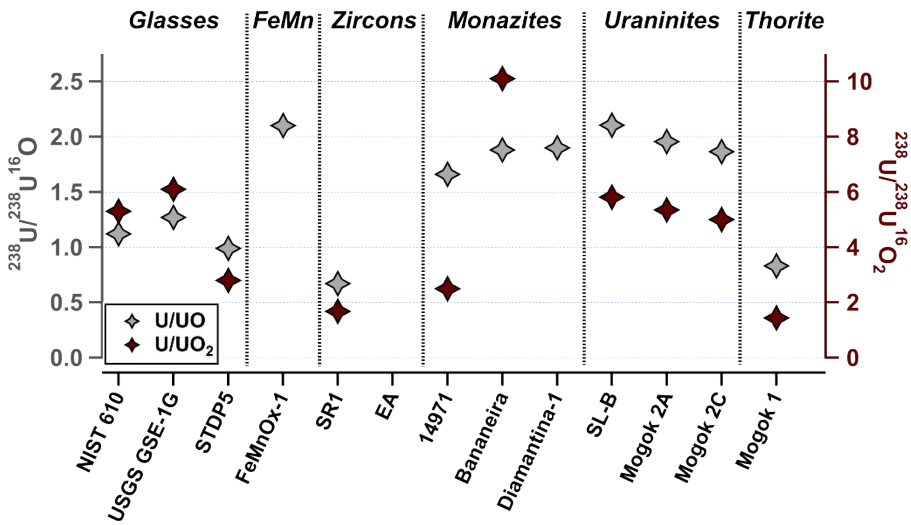

Fig. S1 $^{238}U/^{238}U^{16}O$ and $^{238}U/^{238}U^{16}O_2$ ratios measured with the EUV TOF in the different matrices. Note that ratios are not shown for EA because ^{238}U has a large interference in this sample.

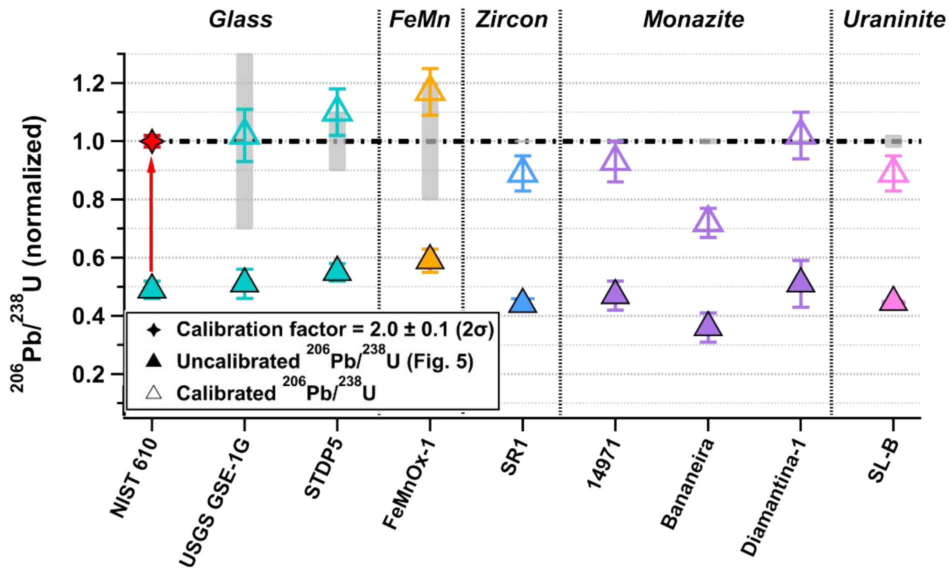

Fig. S2 Uncalibrated and calibrated $^{206}Pb/^{238}U$ ratios (normalized to 1) measured with the EUV TOF. The direct uncalibrated (i.e., raw) $^{206}Pb/^{238}U$ ratios are from Fig. 5 and are shown as solid triangles. The open triangles represent calibrated $^{206}Pb/^{238}U$ ratios using the NIST 610 CRM as the calibration standard, where the calibration factor is 2.0 ± 0.1 (2σ). The error bars on each point are ±2σ. The black dotted line represents the expected normalized ratios (i.e., 1). The gray bars are the corresponding ±2σ uncertainty for the expected ratios. The Mogok uraninites and thorite are not shown on this plot because they significantly deviate from the expected values by >50% when the calibration factor is applied.

References

1. C. Kaiyun, Y. Honglin, B. Zhian, Z. Chunlei and D. Mengning, *Geostand. Geoanalytical Res.*, 2013, **38**, 5-21.
2. I. Nikogosian, Ö. Ersoy, M. Whitehouse, P. R. D. Mason, J. C. M. de Hoog, R. Wortel and M. J. van Bergen, *Earth Planet. Sci. Lett.*, 2016, **449**, 12-19.
3. G. O. Goncalves, C. Lana, R. Scholz, I. S. Buick, A. Gerdes, S. L. Kamo, F. Corfu, M. M. Marinho, A. O. Chaves, C. Valeriano and H. A. Nalini Jr., *Chem. Geol.*, 2016, **424**, 30-50.
4. G. O. Goncalves, C. Lana, R. Scholz, I. S. Buick, A. Gerdes, S. L. Kamo, F. Corfu, D. Rubatto, M. Wiedenbeck, H. A. Nalini Jr. and L. C. A. Oliveira, *Geostand. Geoanalytical Res.*, 2017, **42**, 25-47.